https://doi.org/10.5194/amt-2023-179
Preprint. Discussion started: 21 August 2023

Atmospheric Measurement Techniques Discussions

Multi-wavelength dataset of aerosol extinction profiles retrieved from GOMOS stellar occultation measurements

Viktoria F. Sofieva[1], Monika Szelag[1], Johanna Tamminen[1], Didier Fussen[2], Christine Bingen[2], Filip Vanhellemont[2], Nina Mateshvili[2], Alexei Rozanov[3] and Christine Pohl[3]

[1] Finnish Meteorological Institute, Helsinki, Finland
[2] Royal Belgian Institute for Space Aeronomy (BIRA-IASB), Brussels, Belgium
[3] Institute of Environmental Physics, University of Bremen, Bremen, Germany

Correspondence to: Viktoria Sofieva (viktoria.sofieva@fmi.fi)

Abstract.

In this paper, we present the new multi-wavelength dataset of aerosol extinction profiles, which are retrieved from the averaged transmittance spectra by the Global Ozone Monitoring by Occultation of Stars instrument on board the Envisat satellite.

Using monthly and zonally averaged transmittances as a starting point for the retrievals enables us to improve the signal-to-noise ratio and eliminate possible modulation of transmittance spectra by uncorrected scintillations. The two-step retrieval method is used: the spectral inversion is followed by the vertical inversion. The spectral inversion relies on the removal of contributions from ozone, NO_2, NO_3 and Rayleigh scattering from the optical depth spectra, for each ray perigee altitude. In the vertical inversion, the profiles of aerosol extinction coefficients at several wavelengths are retrieved from the collection of slant aerosol optical depth profiles.

The retrieved aerosol extinction profiles (FMI-GOMOSaero dataset v1) are provided in the altitude range 10-40 km at wavelengths 400, 440, 452, 470, 500, 525, 550, 672 and 750 nm, for the whole GOMOS operating period from August 2002 to March 2012.

The retrieved aerosol extinction profiles show a realistic wavelength dependence. Intercomparisons have shown that FMI-GOMOSaero aerosol profiles are in good agreement with other datasets and have suggested a better data quality compared to the previous GOMOS aerosol data.

1 Introduction

Stratospheric aerosols impact the radiative forcing and thus the energy balance of the Earth's atmosphere, therefore information about their distribution and variability is of high importance for climate related studies. The stellar occultation instrument GOMOS (Global Ozone Monitoring by Occultation of Stars) , which operated on the Envisat satellite in 2002-2012, was capable of providing the profiles of aerosol extinction coefficient in the altitude range from ~10 to 40 km (Kyrölä

https://doi.org/10.5194/amt-2023-179
Preprint. Discussion started: 21 August 2023


Atmospheric Measurement Techniques Discussions

et al., 2010; Bertaux et al., 2010; Vanhellemont et al., 2010). The GOMOS aerosol data have already been used in the merged stratospheric aerosol dataset (Vernier et al., 2011) and climate studies (Solomon et al., 2011; Santer et al., 2014; Brühl et al., 2018; Schallock et al., 2021), and to produce reference climate data records (Popp et al., 2016; Bingen et al., 2017).

GOMOS was equipped with UV-VIS (250 - 690 nm) and IR (755-774 nm and 926-954 nm) grating spectrometers operating at a sampling frequency of 2 Hz, and with two fast photometers at ~472 nm and ~672 nm operating at 1 kHz sampling frequency. GOMOS measured stellar irradiance in the limb-viewing geometry from ~140 km down to full extinction at about 10-15 km (Bertaux et al., 2010). The transmittance spectra are obtained after dividing the stellar spectra observed through the atmosphere by the reference spectrum above the atmosphere. After correction of refraction effects (refractive attenuation and scintillation), the transmittance spectra are the basis for retrievals of trace gases and aerosol extinction.

The GOMOS IPF (Instrument Processor Facility) v6 retrievals of ozone, NO_2, NO_3 and aerosol extinction rely on two-step inversion (Kyrölä et al., 2010). First, the horizontal column densities are retrieved from transmittance spectra $T(\lambda,z)$ for each tangent altitude (the spectral inversion). After that, the local density profiles are obtained from the profiles of horizontal column densities (the vertical inversion). In the IPF spectral inversion, the contribution due to Rayleigh scattering is estimated using the ECMWF data, and horizontal column densities of ozone, NO_2, NO_3 and aerosol extinction are retrieved simultaneously from UV-VIS spectrometer data, with iterative DOAS-type inversion for NO_2 and NO_3. Since the spectral dependence of aerosol cross-sections, which depend on particle size distribution, is not known, the IPF v6 processor uses a parameterization via a second-degree polynomial model in wavelength λ (Kyrölä et al., 2010; Vanhellemont et al., 2010). The GOMOS IPF v6 processor provides the aerosol extinction coefficient data record at 500 nm and its spectral dependence, expressed by the coefficients of the polynomial mentioned above.

In the AERGOM processor, which is optimized for aerosol retrievals (Vanhellemont et al., 2016), the data from the spectrometer B1 (755-774 nm) are also used together with the UV-VIS spectrometer data for retrievals of aerosol extinction. In AERGOM, the spectral dependence of aerosol extinction is parameterized by a second-degree polynomial in $1/\lambda$. As in IPF v6, the retrievals are performed in two steps, the non-linear spectral inversion is followed by the linear vertical inversion. In the AERGOM spectral inversion, horizontal column densities of ozone, NO_2, NO_3 and aerosol extinction are retrieved simultaneously from UV-VIS spectrometer data. Covariances between species after the spectral inversion are taken into account in AERGOM, while they are neglected in the IPF v6 processor. AERGOM performs the vertical inversion for all species simultaneously, while the IPF v6 processor does it for each species separately, with a decreased information content. Finally, for aerosol extinction, AERGOM applies three altitudinal regularization constraints (at three wavelenghs), while IPF v6 applies only one (aerosol extinction at 500 nm). From all AERGOM vertical aerosol extinction coefficient profiles, a 5-days gridded climate data record was set up with a spatial resolution of 5° latitude and 60° longitude was created (Bingen et al., 2017). This climate data record, which is referred to as CCI-AerGOM and is available at https://cds.climate.copernicus.eu/cdsapp#!/dataset/10.24381/cds.239d815c?tab=form, contains the profiles of average aerosol extinction coefficient at 355, 440, 470, 550 and 750 nm.

https://doi.org/10.5194/amt-2023-179
Preprint. Discussion started: 21 August 2023

Atmospheric Measurement Techniques Discussions

Although GOMOS aerosol extinction coefficient data are available from the ESA IPF v6 and AERGOM processors, the reported spectral dependence of the aerosol extinction is often not realistic, mainly due to interference with ozone retrievals, limited wavelength range in the IPF v6 retrievals, insufficient signal-to-noise ratio, residual scintillation and the limitations of the polynomial model. In particular, it is known that lower stratospheric ozone in IPF v6 has a strong bias, and this influences the quality of aerosol retrievals, as ozone and aerosols are retrieved simultaneously. The AERGOM aerosol extinction was reported to show a negative bias above 25 km altitude for wavelengths larger than 700 nm (Robert et al., 2016).

In this paper, we aim at addressing these issues by using averaged GOMOS transmissions to create a multi-wavelength aerosol extinction profile dataset (climate data record) from averaged GOMOS transmittances. The proposed new algorithm for aerosol retrievals is based on the removal of extinctions due to the Rayleigh scattering and absorption by ozone and other trace gases from GOMOS transmission spectra.

The paper is organized as follows. Section 2 describes the inversion algorithm. The retrieval results and various intercomparisons are presented in Section 3. Section 4 is dedicated to characterization of the entire retrieved GOMOS aerosol dataset as a climate data record. The summary and discussion (Section 5) concludes the paper.

2 The inversion algorithm

2.1 Preparation for retrievals: creating averaged transmittances dataset

The monthly averaged transmittances $T(\lambda, z)$ as function of wavelength λ and tangent altitude z are used as a starting point for the retrievals. The self-calibrating property of the occultation method suggests averaging of independent observations for the sake of augmenting their statistical significance. This technique allows for the detection of very weak absorbers (e.g., OClO (Fussen et al., 2006) or Na (Fussen et al., 2010)), as it increases the signal-to-noise ratio. Furthermore, the level of the stochastic residual scintillations is greatly reduced.

For computing averaged transmittances, we used GOMOS nighttime measurements (i.e., with a solar zenith angle at the ray perigee point larger than 107°). The refractive effects - refractive dilution and perturbations due to scintillations - are estimated and removed from the transmittance spectra, for each occultation (Dalaudier et al., 2001; Sofieva et al., 2009; Kyrölä et al., 2010). The transmittances with removed refractive effects (EXT product) are used in our computations. The methodology for computing the GOMOS averaged transmittances has been developed in the dedicated ESA project ALGOM (https://earth.esa.int/eogateway/activities/algom). It includes interpolation of transmittances at a fixed altitude grid, outlier filtering, and data averaging. The outlier filtering is performed using an algorithm based on the well-known Jackknife method (e.g., Miller, 1974). The threshold for outliers has been chosen as 3 standard deviations from the median.

For each tangent altitude and each wavelength, the average transmittance is computed as the weighted median transmittance. This estimate is insensitive to outliers, and it takes into account the signal-to-noise ratio of different measurements, which

https://doi.org/10.5194/amt-2023-179
Preprint. Discussion started: 21 August 2023

Atmospheric Measurement Techniques Discussions

can differ considerably for GOMOS due to different stellar sources. The transmittances are weighted with respect to the inverse of their estimated measurements errors.

A classical definition of the weighted median was used (Edgeworth, 1888). Technically, it was computed as a central element of a sorted set, in which values are replicated according to their relative weights.

The examples of averaged transmittances for the latitude bin 0-10°N are shown in Figure 1, for conditions of a low loading level (January 2003, left panel of Figure 1) and increased aerosols after Soufrière Hills, Rabaul and Tavurvur volcanic eruptions (January 2007, right panel). It is clearly seen that the transmittances are lower (optical depth is higher) for the volcanic aerosol conditions (compare transmittances at 20 km, thick red lines).

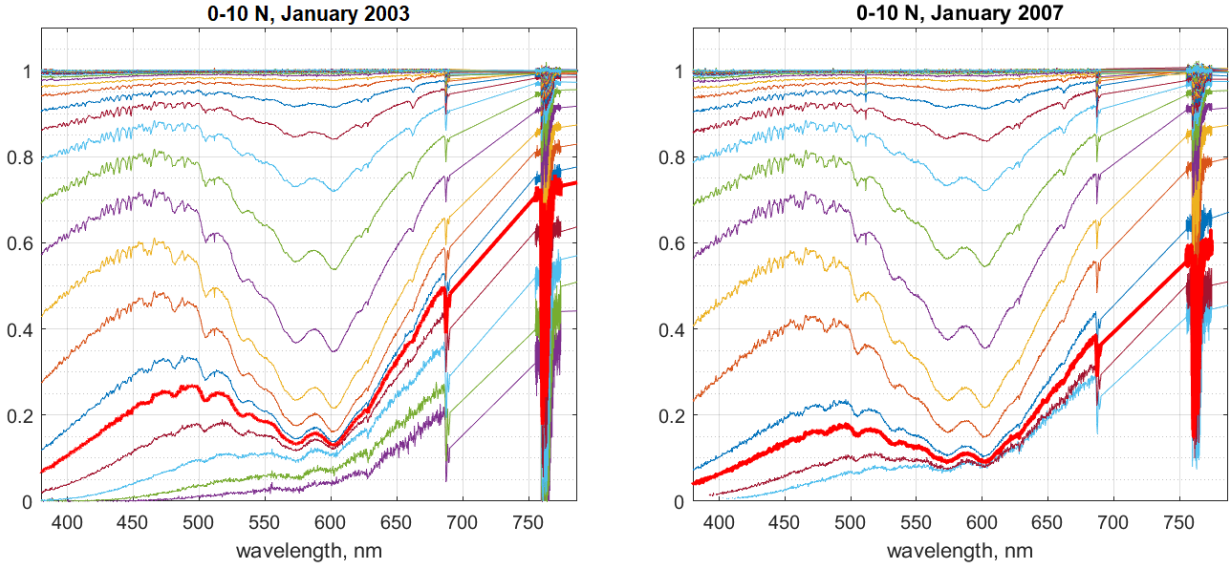

Figure 1. Examples of GOMOS averaged transmittance spectra in the equatorial region 0-10°N, in January 2003 (background aerosols) and in January 2007 (after volcanic eruptions). Red thick lines highlight transmittances at 20 km. For visibility, the transmittance spectra are plotted with the vertical step of 3 km.

2.2 Aerosol retrieval algorithm

The idea of aerosol retrievals from averaged transmittances with removed refractive effects is very simple. If the extinction due to Rayleigh scattering and due to absorption by ozone, NO_2 and NO_3 can be removed from the GOMOS extinction spectra, the remaining part is due to aerosol extinction.

We used data from spectrometer A at wavelengths 380-672 nm and spectrometer B1 at wavelengths 755-759 nm. The NO_2 and NO_3 optical depths are computed using retrieved GOMOS NO_2 and NO_3 profiles, which are averaged in the

https://doi.org/10.5194/amt-2023-179
Preprint. Discussion started: 21 August 2023

Atmospheric Measurement Techniques Discussions

corresponding month and latitude bin. The Rayleigh extinction is computed using ECMWF air density data provided in the GOMOS files, which are averaged in the same way. As in ALGOM2S retrievals (Sofieva et al., 2017), ozone optical depth is computed using a DOAS-type retrieval with the triplet in the Chappuis band (reference wavelengths: 523 – 527 nm, 673–677 nm and absorbing wavelengths: 598–602 nm). In the processing, we filtered out unreliable averaged transmittance values (with estimated uncertainties exceeding 100 %).

The details of the retrieval of horizontal aerosol optical depth are illustrated in Figure 2 for the altitude of 20 km near the Equator (0°-10°S). The measured total optical depth, $\tau(\lambda, z) = -\log(T)$, is shown by the black line. The estimated optical depths due to ozone (τ_{ozone}), NO2(τ_{NO_2}), NO3(τ_{NO_3}) and Rayleigh extinction (τ_{air}) are shown by colored lines in the upper panel of Figure 2.

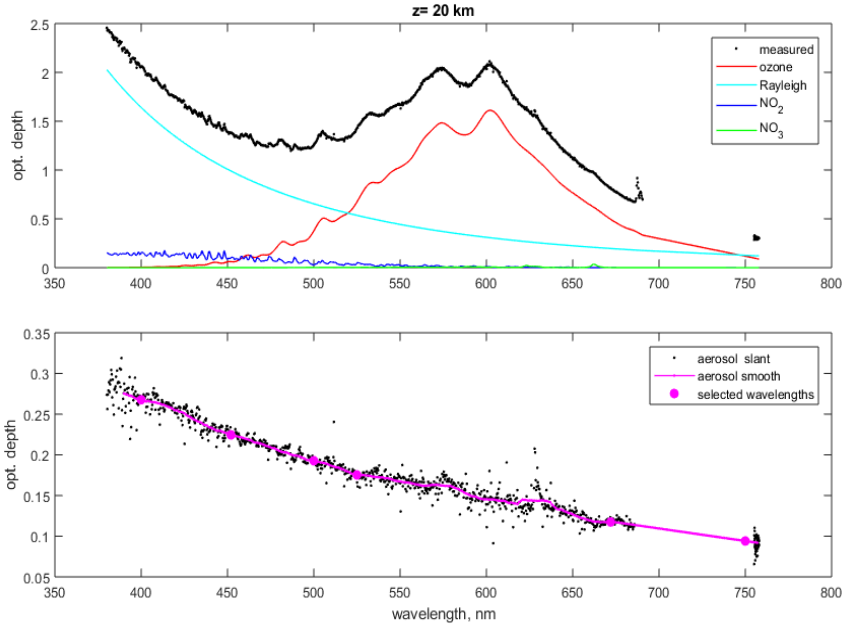

Figure 2. Illustration of the GOMOS aerosol retrieval algorithm. Top: measured optical depth spectrum (black) and contributions due to ozone (red), Rayleigh scattering (cyan), NO2 (blue) and NO3(green). Bottom: original (black) and smoothed (magenta) residuals.

The resulting residuals

$$R(\lambda, z) = \tau(\lambda, z) - \tau_{ozone}(\lambda, z) - \tau_{air}(\lambda, z) - \tau_{NO_2}(\lambda, z) - \tau_{NO_3}(\lambda, z) \quad (1)$$

are due to aerosols. The residual spectra are smoothed and sampled at 9 wavelengths (400, 440, 452, 470, 500, 525, 550, 672 and 750 nm), resulting in the horizontal aerosol optical depth spectra $\tau_{aero}(\lambda, z)$ at each tangent altitude. The wavelengths are selected to be as used by other instruments/retrievals.

https://doi.org/10.5194/amt-2023-179
Preprint. Discussion started: 21 August 2023

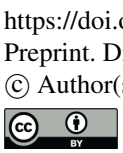

Atmospheric Measurement Techniques Discussions

In the vertical inversion, the profiles of local aerosol extinction coefficients are reconstructed from the horizontal aerosol optical depth profiles $\tau_{aero}(\lambda, z)$, for each wavelength. The GOMOS vertical inversion is linear, and it is performed in the same way as in the GOMOS processor (Kyrölä et al., 2010). The target-resolution Tikhonov-type regularization is applied in the vertical inversion (Sofieva et al., 2004; Kyrölä et al., 2010). The resulting actual altitude resolution of the aerosol extinction profiles $\beta(\lambda, z)$ is 3 km. The uncertainties of retrieved aerosol extinction profiles are estimated via error propagation of transmittance uncertainties. Typical uncertainties of the retrieved aerosol profiles are shown in Figure 4.

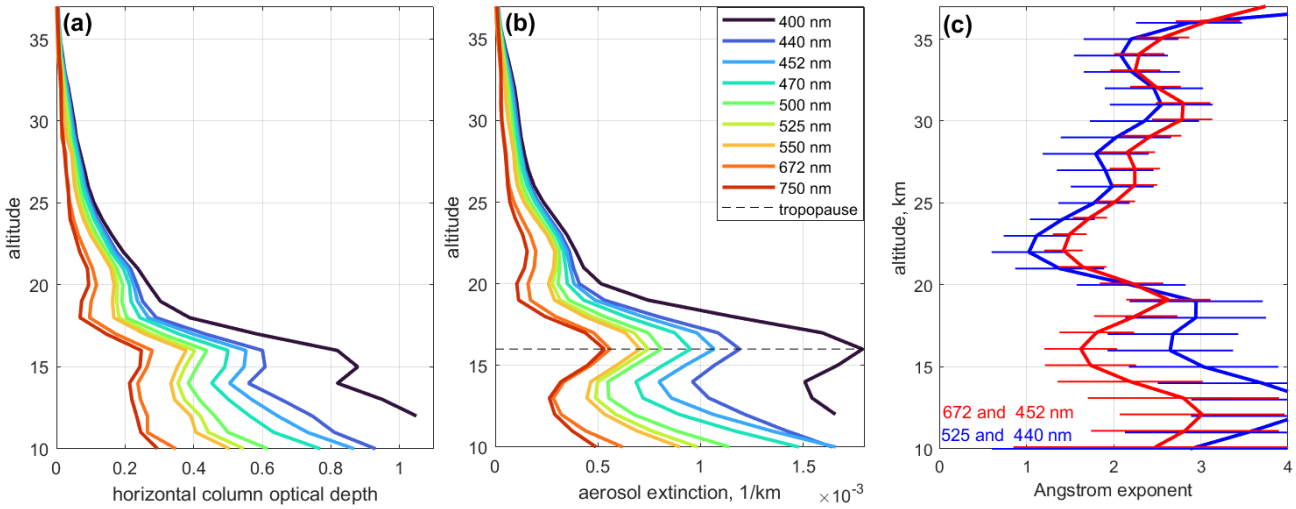

Figure 3. The retrieved horizontal column optical depth (panel a) and aerosol extinction (panel b) for September 2002, 10°-20° S (wavelengths are indicated in the legend). Panel (c): the Ångström exponent profiles estimated using different combinations of wavelengths. The mean tropopause height is indicated by black dashed line on panel (b).

Examples of retrieved horizontal column optical depth and aerosol extinction profiles are shown in Figure 3**.** One can notice the expected spectral dependence of aerosol extinction that is larger for shorter wavelengths. The profiles of the Ångström exponent

$$\alpha = -\frac{log(\frac{\beta(\lambda)}{\beta(\lambda_0)})}{log(\frac{\lambda}{\lambda_0})} \quad (2)$$

for different wavelength combinations are shown in Figure 3c. The uncertainties of Ångström exponent are evaluated from uncertainties of retrieved aerosol profiles via error propagation. The values of the Ångström exponent are in the expected range from 0-0.5 (large particles) to 4 (Rayleigh scattering limit). Above ~22 km, α grows with altitude becoming closer to the Rayleigh scattering limit, as expected. Below 20 km, the Ångström exponent estimates have large uncertainties,

https://doi.org/10.5194/amt-2023-179
Preprint. Discussion started: 21 August 2023


Atmospheric Measurement Techniques Discussions

especially when using short wavelengths (example of 525 and 440 nm in Figure 3c). The Ångström exponent estimated using 672 and 452 nm are in the range 1.5- 3 below 20 km.

3 Retrieval results and intercomparisons

The multi-wavelength FMI-GOMOSaero aerosol retrievals can be directly compared with data from other instruments.

In addition to other GOMOS datasets (IPF v6 and AERGOM), we compare our retrievals with aerosol data from SAGE II (Stratospheric Aerosol and Gas Experiment II) on the Earth Radiation Budget Satellite, OSIRIS (Optical Spectrograph and InfraRed Imaging System) on Odin and SCIAMACHY (SCanning Imaging Spectrometer for Atmospheric CHartographY) on Envisat. The aerosol datasets used for intercomparisons are described in Table 1.

Table 1. Aerosol datasets used for intercomparisons

Instrument	Retrieval methods/data	Retrieved aerosol parameter(s)	References
SAGE-II v.7 1984-2005	Transmittances UV-VIS-IR	Aerosol extinction at 386, 452, 525 and 1020 nm	(Thomason et al., 2008)
GOMOS AERGOM v.4 2002-2011	Transmittances in UV VIS-NIR	Aerosol extinction at 355, 440, 470, 550 and 750 nm, aerosol size distribution	(Vanhellemont et al., 2016; Bingen et al., 2017)
OSIRIS v.6 (2001-present)	Radiances at 470, 750 and 1530 nm	Aerosol extinctions at 750 nm, the mode radius	(Rieger et al., 2014)
SCIAMACHY UBR v.3.0 (2002-2012)	Sun-normalized radiance at 750 nm, effective surface albedo from collocated nadir measurements SCIATRAN + non-liner regularized inversion	Aerosol extinction at 750 nm	The precursor retrieval version V1.4 is published in (von Savigny et al. 2015) and (Ernst et al., 2012)
SCIAMACHY UBR PSD v2.0 retrievals (2002-2012)	Sun-normalized radiances in UV-VIS-IR, effective surface albedo from collocated nadir measurements SCIATRAN + non-liner regularized	Particle size distribution	(Pohl et al., 2023)

https://doi.org/10.5194/amt-2023-179
Preprint. Discussion started: 21 August 2023

Atmospheric Measurement Techniques Discussions

	inversion		

For the comparisons, the individual aerosol profiles from SAGE II, OSIRIS, SCIAMACHY and AERGOM are averaged to create monthly zonal mean data. Figure 4 shows the comparison of GOMOS and SAGE II aerosol extinction profiles at 525 nm in September 2002 at latitudes 10°-20°S. One can observe a very good agreement with SAGE II above 20 km. Below 20 km GOMOS aerosol extinction is larger, but it is in a good agreement with SAGE II extinction with omitted cloud filtering (compare magenta and blue lines in Figure 4). When using averaged transmittances, cirrus clouds cases cannot be excluded, which might result in overestimation of the aerosol extinction below 20 km (see also the discussion below). Figure 5 shows the GOMOS and monthly mean cloud-filtered SAGE II aerosol profiles for the same latitude bin at several wavelengths. Although the spectral dependence of aerosol extinction profiles is similar above 20 km, it differs below 20 km.

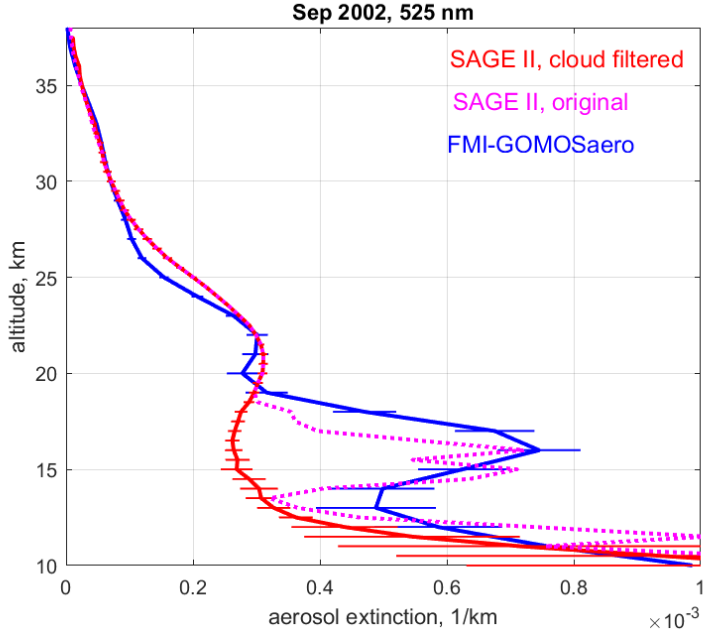

Figure 4. Comparison of GOMOS and SAGE II monthly mean aerosol extinction profiles at 525 nm, September 2002, 10°-20° S. Uncertainties of FMI-GOMOS aero are computed in the retrievals (see text for explanation). Uncertainties of SAGE II data are estimated as a standard error of the mean.

https://doi.org/10.5194/amt-2023-179
Preprint. Discussion started: 21 August 2023

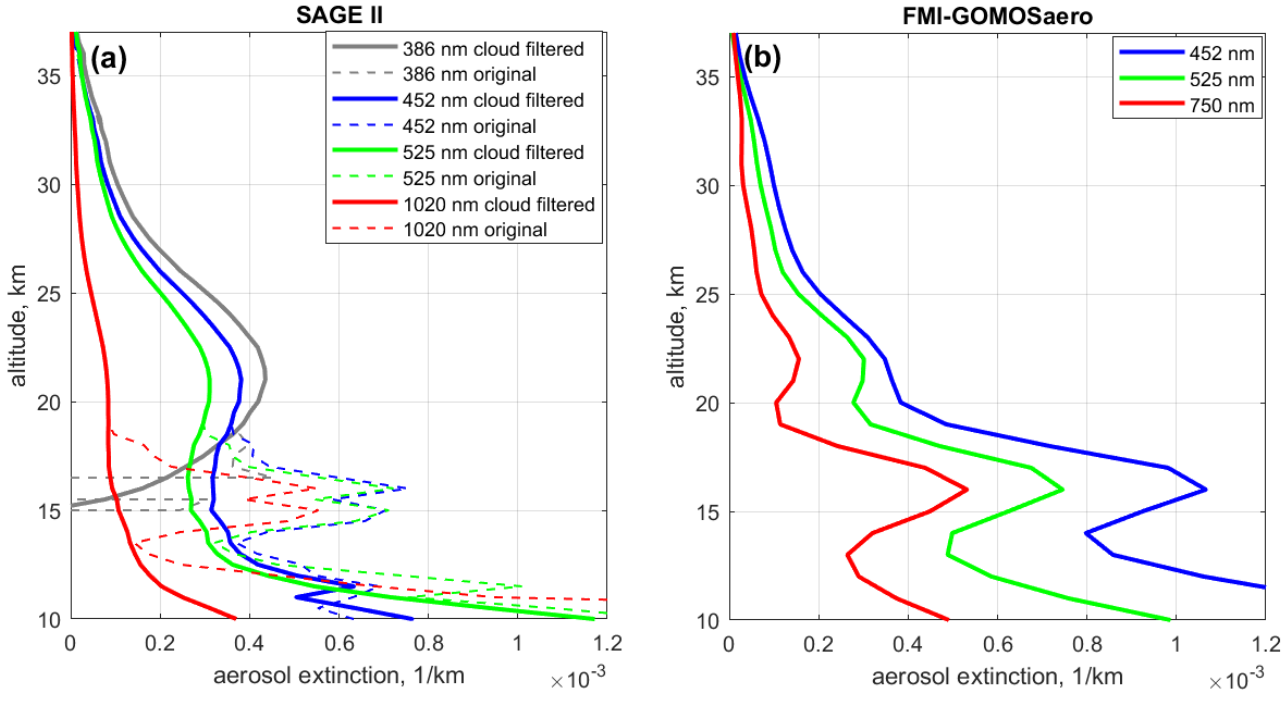

Figure 5 Comparison of FMI-GOMOSaero (panel b) and SAGE II (panel a) monthly mean aerosol profiles at several wavelengths, September 2002, 10°-20° S. The wavelengths are specified in the legend. For SAGE II, profiles with (solid lines) and without cloud filtering (dashed lines) are shown.

Figure 6 shows FMI-GOMOSaero and the monthly average AERGOM aerosol extinction profiles in the same latitude band 10°-20° S, in September 2002. The uncertainties of AERGOM monthly mean data are estimated as the standard error of the mean. We also computed the Ångström exponent profiles using two combinations of wavelength: 550 and 440 nm, and 750 and 550 nm (Figure 6c). Above 20 km, the aerosol extinction profiles and their spectral dependence are rather similar in both datasets. The Ångström exponent profiles computed using aerosol extinction at 750 and 550 nm are close in FMI-GOMOSaero and AERGOM. At shorter wavelengths (Figure 6c, lines for 550 and 440 nm), AERGOM Ångström exponent is ~1 there, while FMI-GOMOSaero analogous values are somewhat larger, in the range ~1-3, increasing with altitude. Below 20 km, the spectral dependence shows different behaviour: in our retrievals, aerosol extinction is larger for shorter wavelengths, while the opposite behavior is observed in AERGOM data. Although the spectral dependence is expected to be decreasing or flat depending on the particle size distribution, the uncertainties of AERGOM at short wavelengths are very large and they explain this unexpected behavior. Figure 6c, Ångström exponent is not shown below 18 km, where its uncertainty (computed via error propagation) exceeds 150 %.

https://doi.org/10.5194/amt-2023-179
Preprint. Discussion started: 21 August 2023

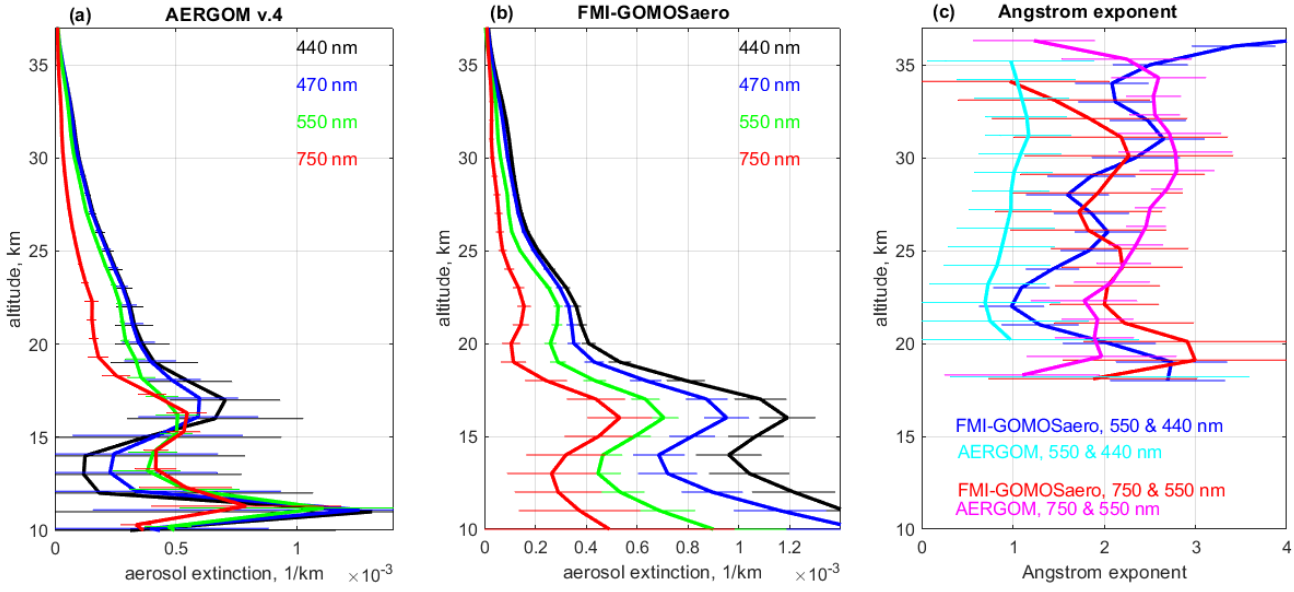

Figure 6. AERGOM (left) and new GOMOS (center) aerosol extinction profiles at several wavelengths. Right: profiles of the Ångström exponent. The data are for September 2002, 10°-20° S. The profiles are shown with 1σ uncertainties. Ångström exponent values with uncertainty exceeding 150% are not shown in panel (c).

Figure 7 compares FMI-GOMOSaero profiles for September 2002 in the latitude zone 10°-20°S, with the averaged profiles from several satellite instruments. At 525 nm, our retrievals are compared with AERGOM (at 550 nm), SAGE II, and SCIAMACHY measurements. At 750 nm, our new GOMOS aerosol profile is compared with AERGOM, SCIAMACHY and OSIRIS data. In both comparisons, the SCIAMACHY data from the special retrievals with the reconstruction of the particle size distribution (Malinina et al., 2018; Pohl et al., 2023) are used (cyan lines). The blue line in the right panel of Figure 7 corresponds to nominal SCIAMACHY UBr v3.0 retrievals. In general, GOMOS aerosol extinction profiles are very close to those of other instruments above 20 km. The best agreement is with SAGE II and OSIRIS data. At lower altitudes, the GOMOS aerosols are biased toward larger values. This feature is present in our retrievals and also in the AERGOM dataset.

The reason for positive bias near the tropical tropopause is GOMOS aerosol retrievals is not fully understood at the moment. Comparison with SAGE II data without additional cloud filtering (Figure 4) suggests that a possible reason could be very thin cirrus clouds, which are very difficult to separate from aerosols.

We tried to apply various methods for cloud filtering in averaging GOMOS transmittances– according to absolute values of extinction and ratio at different wavelengths. However, the effect is rather minor. We also investigated another hypothesis - imperfect refractive dilution correction due to inaccurate ECMWF data (note that very old ECMWF forecast data have been used in the GOMOS processor). Although some improvement is observed when ERA-5 data are used, it does not

https://doi.org/10.5194/amt-2023-179
Preprint. Discussion started: 21 August 2023

Atmospheric Measurement Techniques Discussions

completely remove the enhancements in the retrieved aerosol extinction near the tropical tropopause. In addition, the GOMOS dilution is estimated using a first-order approximation (Dalaudier et al., 2001), which might be not accurate in the vicinity of the tropical tropopause.

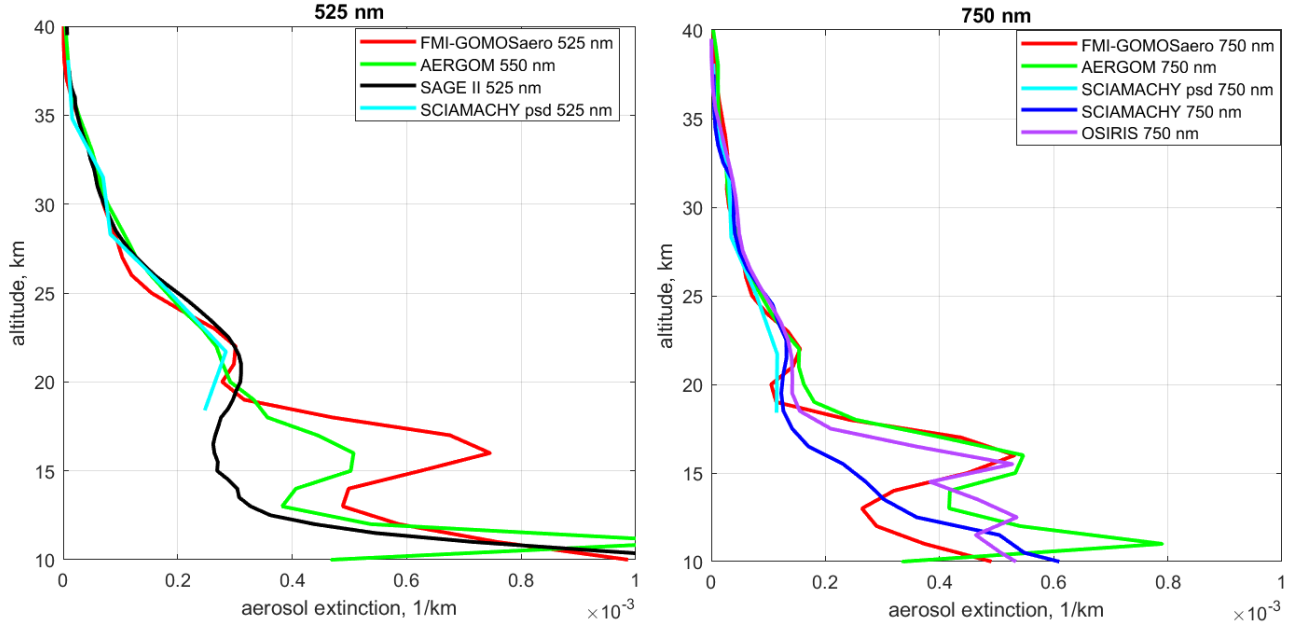

Figure 7. Comparison of new GOMOS retrieved profiles for September 2002, 10-20 S, with data from several satellite instruments. Left panel: comparisons for the wavelength 525 nm, right panel: comparisons for the wavelength 750 nm.

4 FMI-GOMOSaero aerosol climate data record

The entire GOMOS dataset has been processed. Subsequently, we filtered out the data points that have unrealistic values for the Ångström exponent (α>4 below 27 km) or are potentially affected by clouds (α<-0.2).

By examining outliers in the processed GOMOS-FMI aerosol dataset we found that one of the reasons for strong outliers is an insufficient amount of data available for transmittance averaging. Therefore, the data based on a small number of averaged transmittances (less than 20) are excluded from the final GOMOS aerosol dataset.

Figure 8 shows the time series of stratospheric aerosol extinction at 20 km for 3 wavelengths: 525nm, 672 nm and 750 nm. Main aerosol events (volcanic eruptions and wild fires) in 2002-2012 (see Table 2) are indicated in Figure 8 by black circles of the size proportional to their volcanic explosivity index VEI. Volcanic eruption signatures are clearly seen in 2007, 2009 and 2010. The time series for 672 nm and 750 nm look similar, suggesting a similar data quality.

https://doi.org/10.5194/amt-2023-179
Preprint. Discussion started: 21 August 2023

Atmospheric Measurement Techniques Discussions

235

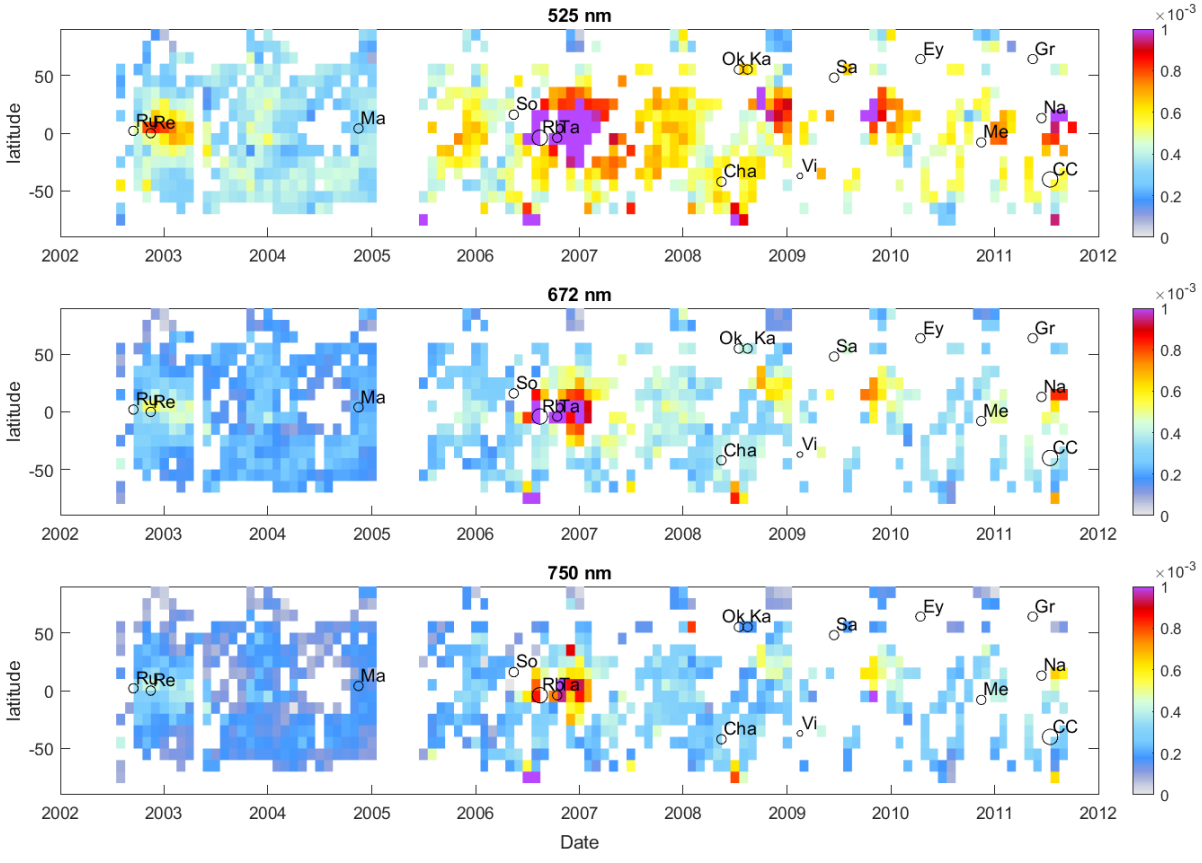

Figure 8. Time series of aerosol extinction(1/km) at 20 km for 525 nm (top), 672 nm (center) and 750 nm (bottom). Main aerosol events (volcanic eruptions and wild fires) are indicated by black circles of the size proportional to their volcanic explosivity index VEI.

240

Table 2. The list of volcanic eruptions and strong wildfires.

year	month	Volcano/wildfire name	Abbreviation	Latitude (deg North)	VEI
2002	9	Ruang	Ru	2	4
2002	11	Reventador	Re	0	4
2004	11	Manam	Ma	4	4
2006	5	Soufrière Hills	So	16	4

https://doi.org/10.5194/amt-2023-179
Preprint. Discussion started: 21 August 2023

Atmospheric Measurement Techniques Discussions

2006	8	Rabaul	Rb	-4	5
2006	10	Tavurvur	Ta	-4	4
2008	5	Chaitén	Cha	-42	4
2008	7	Okmok	Ok	55	4
2008	8	Kasatochi	Ka	55	4
2009	2	Fire/Victoria	Vi	-37	3
2009	6	Sarychev	Sa	48	4
2010	4	Eyjafjallajokull	Ey	64	4
2010	11	Merapi	Me	-8	4
2011	5	Grimsvótn	Gr	64	4
2011	6	Nabro	Na	13	4
2011	7	Cordon Caulle	CC	-40	5

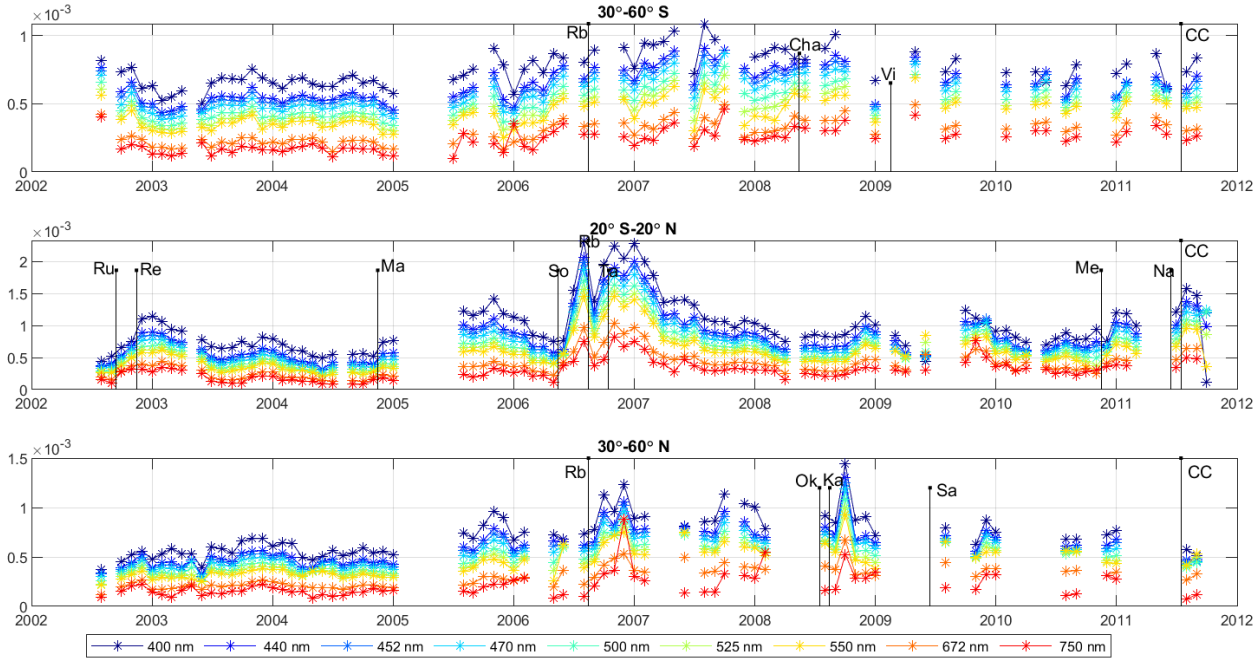

Figure 9. Time series of GOMOS-FMI aerosol extinction (1/km) at 20 km in the latitude zones 30°-60° S (top), 20°S-20°N (center) and 30°-60° N (bottom). The wavelengths are indicated in the figure legend. The volcanos are indicated by black bars with the length proportional to volcanic explosivity index (VEI). Volcanos with VEI>=5 are shown for all latitude zones, and with VEI>3 in the corresponding latitude zones.

https://doi.org/10.5194/amt-2023-179
Preprint. Discussion started: 21 August 2023

Atmospheric Measurement Techniques Discussions

Figure 9 shows the time series of aerosol extinction at 20 km in the latitude zones 30°-50° S (top), 20°S-20°N (center) and 30°-50° N (bottom), for all retrieved wavelengths. Aerosol extinction coefficient decrease with wavelength. The enhancements due to volcanic eruptions – Reventador in 2002, Soufrière Hills, Rabaul and Tavurvur in 2006, and Okmok and Kasatochi in 2008 - are seen in the data.

Figure 10 shows an analogous time series of aerosol extinction as shown in Figure 9, but using AERGOM v4 data. The AERGOM data are filtered in the same way as FMI-GOMOSaero and shown for the same latitude-time bins that are present in FMI-GOMOSaero dataset. The time series of AERGOM data without additional filtering (i.e., based on data which are reported as valid in the AERGOM files) is shown in the Supplement (Figure S1). AERGOM aerosol extinction spectra have sometimes an unrealistic shape after 2009 (i.e., extinction does not decrease with wavelength). Furthermore, AERGOM often reports negative aerosol extinction at 440 nm and 750 nm, especially after 2009 (however, the retrieval uncertainties characterize well the AERGOM data, as discussed earlier). The enhancements related to volcanic eruptions are visible in AERGOM, but they are less pronounced compared to FMI-GOMOSaero dataset.

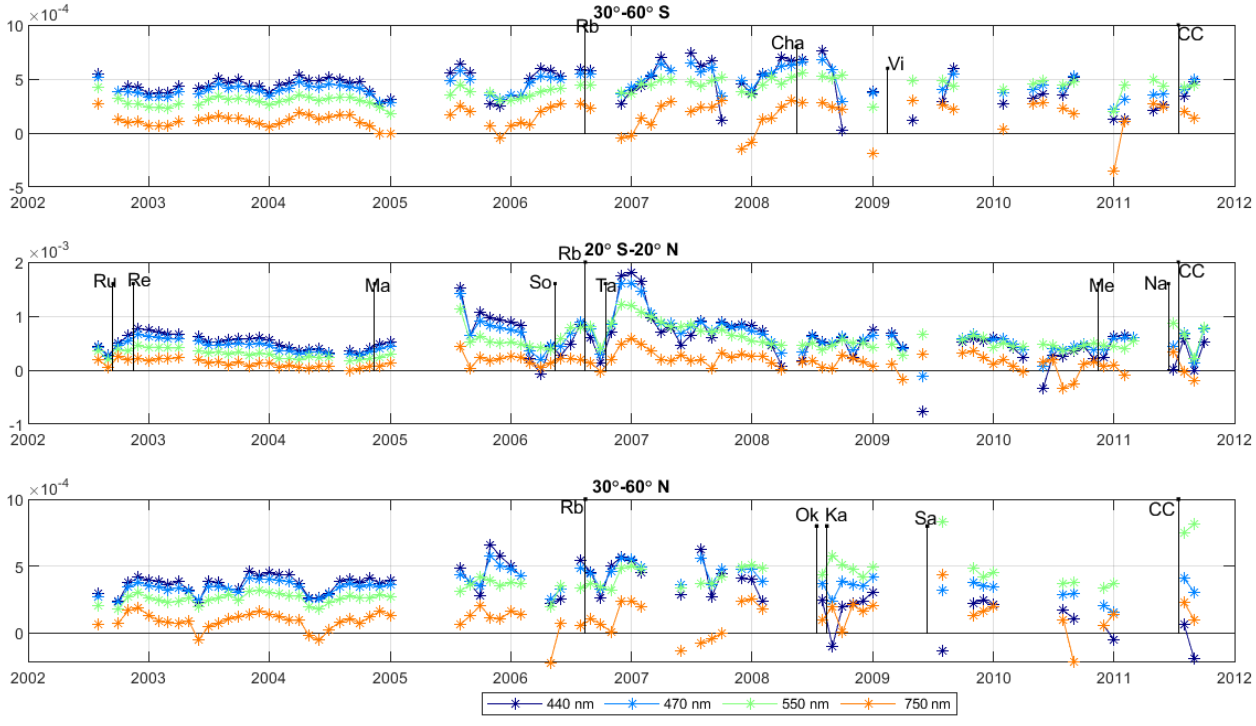

Figure 10. As Figure 9, but for AERGOM v.4 aerosol extinction. AERGOM data are shown only for the same latitude bins and times that are present in FMI-GOMOSaero data.

https://doi.org/10.5194/amt-2023-179
Preprint. Discussion started: 21 August 2023

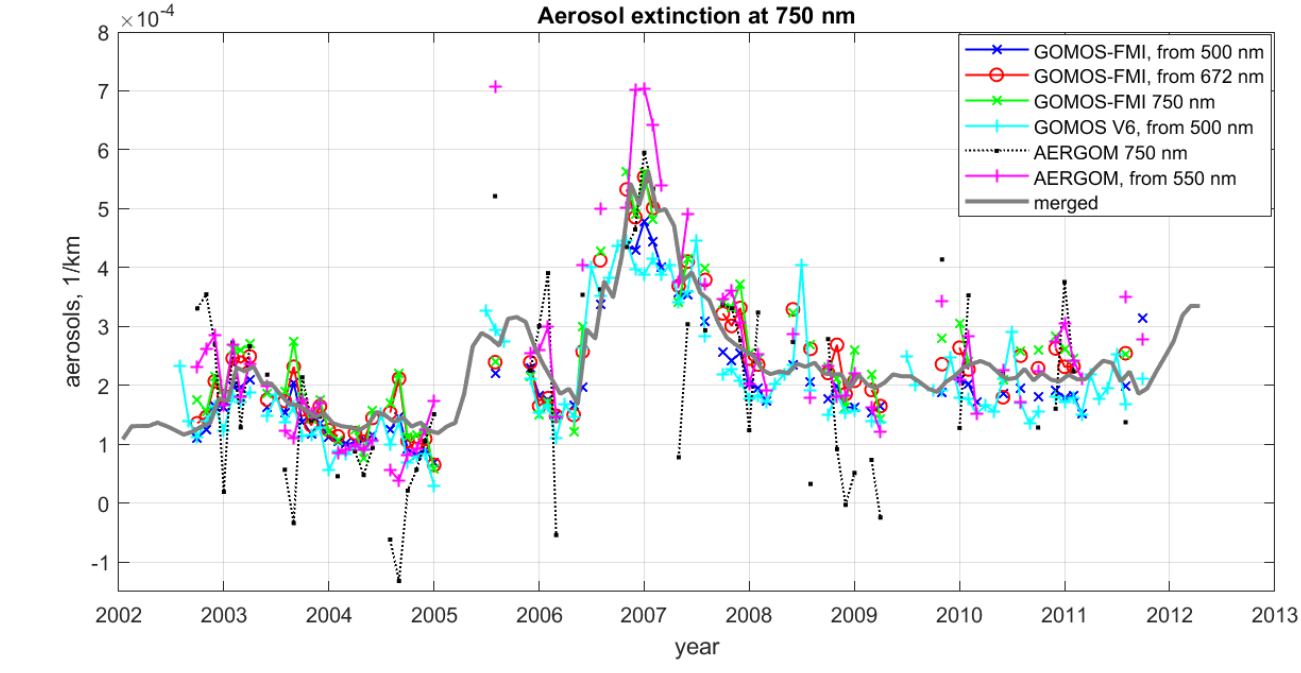

Figure 11. GOMOS aerosol extinction at 750 nm computed by different methods: GOMOS-FMI retrieved at 750 nm (green), GOMOS-FMI converted from 672 nm (red), GOMOS-FMI converted from 500 nm (blue), GOMOS IPF v6 converted from 500 nm (cyan) and AERGOM retrieved at 750 nm(black) and converted from 550 nm (magenta). Thick grey line indicates merged aerosol extinction. All time series are for the latitude bin 0-10°N and altitude 22 km. AERGOM data are shown only for the same latitude bins and times that are present in FMI-GOMOSaero data.

In order to use GOMOS aerosol profile time series in the merged Climate Data of Stratospheric Aerosols, CREST (Sofieva et al: Climate Data Record of Stratospheric aerosols, 2023, in preparation), the data at 750 nm are needed. We have compared the 750 nm GOMOS aerosol extinction time series, computed by different methods: either retrieved at 750 nm or computed from other wavelengths. The latter method was applied using Eq.(2) with the value of Ångström exponent 2.29, a value representative for typical aerosol particle size distributions according to (Malinina et al., 2018). These time series, which are computed using FMI-GOMOSaero aerosols, IPF v6 and AERGOM, are presented in Figure 11, together with the merged aerosol dataset, which is computed as the median of SAGE II, OSIRIS and SCIAMACHY data. In Figure 11, AERGOM data are shown only for the same latitude bins and times that are present in FMI-GOMOSaero. A similar time series but with all AERGOM data reported as valid is shown in the Supplement (Figure S2). We found that the best agreement with the merged aerosol extinction time series is for FMI-GOMOSaero aerosol extinction converted from 672 nm. For using in the merged CREST aerosol climate data record (Sofieva et al., 2023), FMI-GOMOSaero data at 672nm are transformed to 750 nm using the retrieved Ångström exponent.

https://doi.org/10.5194/amt-2023-179
Preprint. Discussion started: 21 August 2023

Atmospheric Measurement Techniques Discussions

5 Summary and discussion

The aerosol retrieval algorithm from averaged transmittance spectra has been developed and applied to the GOMOS night-time dataset. It uses the standard GOMOS two-step retrieval strategy: the spectral inversion is followed by the vertical inversion. The spectral inversion relies on the removal of contributions from ozone, NO_2, NO_3 and Rayleigh scattering from the optical depth spectra, for each ray perigee altitude. The remaining slant optical depth is due to stratospheric aerosols. In the vertical inversion, the profiles of aerosol extinction coefficients at several individual wavelengths are retrieved from the profiles of aerosol horizontal column optical depths.

The new aerosol extinction profiles (FMI-GOMOSaero dataset v.1) are provided in the altitude range 10-40 km at wavelengths 400, 440, 452, 470, 500, 525, 550, 672 and 750 nm. The data are monthly averaged in 10° latitude bands from 90°S to 90°N, for the whole GOMOS operating period from August 2002 to March 2012. The retrieved aerosol extinction profiles show realistic wavelength dependence, and they are in good agreement with other datasets. Aerosol enhancements during volcanic eruptions are clearly seen in FMI-GOMOSaero aerosol time series.

It was demonstrated in the paper that the developed algorithm and the dataset can improve filtering of invalid data in GOMOS aerosol datasets processed by other algorithms. In the future, the developed multi-wavelength dataset of aerosol extinction profiles can be used for retrievals of particle size distribution. The FMI-GOMOSaero monthly mean aerosol extinction profiles can be also used as a-priori information for individual GOMOS retrievals. These developments can be the subject of future works.

Acknowledgements

The work is performed in the framework of ESA project CREST. The creation of the SCIAMACHY aerosol data set at the University of Bremen was funded in parts by ESA via CREST project, by the German Research Foundation (DFG) via the Research Unit VolImpact (grant no. FOR2820), and by the University and State of Bremen. Part of the data processing was done at the German HLRN (High-Performance Computer Center North). The FMI team thanks the Academy of Finland (Centre of Excellence of Inverse Modelling and Imaging; decision 353082)

6 References

Bertaux, J.-L., Kyrölä, E., Fussen, D., Hauchecorne, A., Dalaudier, F., Sofieva, V. F., Tamminen, J., Vanhellemont, F., D'Andon, O. F., Barrot, G., Mangin, A., Blanot, L., Lebrun, J. C., Pérot, K., Fehr, T., Saavedra, L., Leppelmeier, G. W., and Fraisse, R.: Global ozone monitoring by occultation of stars: an overview of GOMOS measurements on ENVISAT, Atmos. Chem. Phys., 10, 12091–12148, https://doi.org/10.5194/acp-10-12091-2010, 2010.

Bingen, C., Robert, C. E., Stebel, K., Brühl, C., Schallock, J., Vanhellemont, F., Mateshvili, N., Höpfner, M., Trickl, T., Barnes, J. E., Jumelet, J., Vernier, J.-P., Popp, T., De Leeuw, G., and Pinnock, S.: Stratospheric aerosol data records for the climate change initiative: Development, validation and application to chemistry-climate modelling, Remote Sensing of Environment, 203, 296–321, https://doi.org/10.1016/j.rse.2017.06.002, 2017.

https://doi.org/10.5194/amt-2023-179
Preprint. Discussion started: 21 August 2023

Brühl, C., Schallock, J., Klingmüller, K., Robert, C., Bingen, C., Clarisse, L., Heckel, A., North, P., and Rieger, L.: Stratospheric aerosol radiative forcing simulated by the chemistry climate model EMAC using Aerosol CCI satellite data, Atmos. Chem. Phys., 18, 12845–12857, https://doi.org/10.5194/acp-18-12845-2018, 2018.

Dalaudier, F., Kan, V., and Gurvich, A. S.: Chromatic refraction with global ozone monitoring by occultation of stars. I. Description and scintillation correction, Applied Optics, 40, 866–877, 2001.

Edgeworth, F. Y.: XXII. *On a new method of reducing observations relating to several quantities*, The London, Edinburgh, and Dublin Philosophical Magazine and Journal of Science, 25, 184–191, https://doi.org/10.1080/14786448808628170, 1888.

Ernst, F., von Savigny, C., Rozanov, A., Rozanov, V., Eichmann, K.-U., Brinkhoff, L. A., Bovensmann, H., and Burrows, J. P.: Global stratospheric aerosol extinction profile retrievals from SCIAMACHY limb-scatter observations, Atmospheric Measurement Techniques Discussions, 5, 5993–6035, https://doi.org/10.5194/amtd-5-5993-2012, 2012.

Fussen, D., Vanhellemont, F., Dodion, J., Bingen, C., Mateshvili, N., Daerden, F., Fonteyn, D., Errera, Q., Chabrillat, S., Kyrölä, E., Tamminen, J., Sofieva, V. F., Hauchecorne, A., Dalaudier, F., Bertaux, J. L., Renard, J.-B., Fraisse, R., d'Andon, O. F., Barrot, G., Guirlet, M., Mangin, A., Théodore, B., P, Snoeij, and Saavedra, L.: A global OClO stratospheric layer discovered in GOMOS stellar occultation measurements, Geophys. Res. Lett., 33, L13815, https://doi.org/10.1029/2006GL026406, 2006.

Fussen, D., Vanhellemont, F., Tetard, C., Mateshvili, N., Dekemper, E., Loodts, N., Bingen, C., Kyrola, E., Tamminen, J., Sofieva, V. F., Hauchecorne, A., Dalaudier, F., Bertaux, J.-L., Barrot, G., Blanot, L., D'Andon, O. F., Fehr, T., Saavedra, L., Yuan, T., and She, C.-Y.: A global climatology of the mesospheric sodium layer from GOMOS data during the 2002-2008 period, ATMOSPHERIC CHEMISTRY AND PHYSICS, 10, 9225–9236, https://doi.org/10.5194/acp-10-9225-2010, 2010.

Kyrölä, E., Tamminen, J., Sofieva, V. F., Bertaux, J.-L., Hauchecorne, A., Dalaudier, F., Fussen, D., Vanhellemont, F., Fanton D'Andon, O., Barrot, G., Guirlet, M., Mangin, A., Blanot, L., Fehr, T., de Miguel, L., and Fraisse, R.: Retrieval of atmospheric parameters from GOMOS data, Atmos. Chem. Phys., 10, 11881–11903, https://doi.org/10.5194/acp-10-11881-2010, 2010.

Malinina, E., Rozanov, A., Rozanov, V., Liebing, P., Bovensmann, H., and Burrows, J. P.: Aerosol particle size distribution in the stratosphere retrieved from SCIAMACHY limb measurements, Atmospheric Measurement Techniques, 11, 2085–2100, https://doi.org/10.5194/amt-11-2085-2018, 2018.

Miller, R. G.: The Jackknife--A Review, Biometrika, 61, 1, https://doi.org/10.2307/2334280, 1974.

Pohl, C., Wrana, F., Rozanov, A., Deshler, T., Malinina, E., Von Savigny, C., Rieger, L. A., Bourassa, A. E., and Burrows, J. P.: Stratospheric aerosol characteristics from SCIAMACHY limb observations: 2-parameter retrieval, Aerosols/Remote Sensing/Data Processing and Information Retrieval, https://doi.org/10.5194/amt-2023-156, 2023.

Popp, T., De Leeuw, G., Bingen, C., Brühl, C., Capelle, V., Chedin, A., Clarisse, L., Dubovik, O., Grainger, R., Griesfeller, J., Heckel, A., Kinne, S., Klüser, L., Kosmale, M., Kolmonen, P., Lelli, L., Litvinov, P., Mei, L., North, P., Pinnock, S., Povey, A., Robert, C., Schulz, M., Sogacheva, L., Stebel, K., Stein Zweers, D., Thomas, G., Tilstra, L., Vandenbussche, S., Veefkind, P., Vountas, M., and Xue, Y.: Development, Production and Evaluation of Aerosol Climate Data Records from European Satellite Observations (Aerosol_cci), Remote Sensing, 8, 421, https://doi.org/10.3390/rs8050421, 2016.

Rieger, L. A., Bourassa, A. E., and Degenstein, D. A.: Stratospheric aerosol particle size information in Odin-OSIRIS limb scatter spectra, Atmospheric Measurement Techniques, 7, 507–522, https://doi.org/10.5194/amt-7-507-2014, 2014.

Robert, C. É., Bingen, C., Vanhellemont, F., Mateshvili, N., Dekemper, E., Tétard, C., Fussen, D., Bourassa, A., and Zehner, C.: AerGOM, an improved algorithm for stratospheric aerosol extinction retrieval from GOMOS observations – Part 2: Intercomparisons, Atmos. Meas. Tech., 9, 4701–4718, https://doi.org/10.5194/amt-9-4701-2016, 2016.

Santer, B. D., Bonfils, C., Painter, J. F., Zelinka, M. D., Mears, C., Solomon, S., Schmidt, G. A., Fyfe, J. C., Cole, J. N. S., Nazarenko, L., Taylor, K. E., and Wentz, F. J.: Volcanic contribution to decadal changes in tropospheric temperature, Nature Geosci, 7, 185–189, 2014.

Schallock, J., Brühl, C., Bingen, C., Höpfner, M., Rieger, L., and Lelieveld, J.: Radiative forcing by volcanic eruptions since 1990, calculated with a chemistry-climate model and a new emission inventory based on vertically resolved satellite measurements, Aerosols/Atmospheric Modelling/Stratosphere/Chemistry (chemical composition and reactions), https://doi.org/10.5194/acp-2021-654, 2021.

Sofieva, V. F., Tamminen, J., Haario, H., Kyrölä, E., and Lehtinen, M.: Ozone profile smoothness as a priori information in the inversion from limb measurements, Ann. Geophysicae, 22, 3411–3420, 2004.

Sofieva, V. F., Kan, V., Dalaudier, F., Kyrölä, E., Tamminen, J., Bertaux, J.-L., Hauchecorne, A., Fussen, D., and Vanhellemont, F.: Influence of scintillation on quality of ozone monitoring by GOMOS, Atmos. Chem. Phys., 9, 9197–9207, 2009.

Sofieva, V. F., Ialongo, I., Hakkarainen, J., Kyrölä, E., Tamminen, J., Laine, M., Hubert, D., Hauchecorne, A., Dalaudier, F., Bertaux, J.-L., Fussen, D., Blanot, L., Barrot, G., and Dehn, A.: Improved GOMOS/Envisat ozone retrievals in the upper troposphere and the lower stratosphere, Atmospheric Measurement Techniques, 10, 231–246, https://doi.org/10.5194/amt-10-231-2017, 2017.

Solomon, S., Daniel, J. S., Neely, R. R., Vernier, J.-P., Dutton, E. G., and Thomason, L. W.: The Persistently Variable "Background" Stratospheric Aerosol Layer and Global Climate Change, Science , 333, 866–870, https://doi.org/10.1126/science.1206027, 2011.

Thomason, L. W., Burton, S. P., Luo, B.-P., and Peter, T.: SAGE II measurements of stratospheric aerosol properties at non-volcanic levels, Atmospheric Chemistry and Physics, 8, 983–995, https://doi.org/10.5194/acp-8-983-2008, 2008.

Vanhellemont, F., Fussen, D., Mateshvili, N., Tetard, C., Bingen, C., Dekemper, E., Loodts, N., Kyrola, E., Sofieva, V. F., Tamminen, J., Hauchecorne, A., Bertaux, J.-L., Dalaudier, F., Blanot, L., D'Andon, O. F., Barrot, G., Guirlet, M., Fehr, T., and Saavedra, L.: Optical extinction by upper tropospheric/stratospheric aerosols and clouds: GOMOS observations for the period 2002-2008, ATMOSPHERIC CHEMISTRY AND PHYSICS, 10, 7997–8009, https://doi.org/10.5194/acp-10-7997-2010, 2010.

Vanhellemont, F., Mateshvili, N., Blanot, L., Robert, C. É., Bingen, C., Sofieva, V. F., Dalaudier, F., Tétard, C., Fussen, D., Dekemper, E., Kyrölä, E., Laine, M., Tamminen, J., and Zehner, C.: AerGOM, an improved algorithm for stratospheric aerosol extinction retrieval from GOMOS observations – Part 1: Algorithm description, Atmospheric Measurement Techniques, 9, 4687–4700, https://doi.org/10.5194/amt-9-4687-2016, 2016.

Vernier, J.-P., Thomason, L. W., Pommereau, J.-P., Bourassa, A., Pelon, J., Garnier, A., Hauchecorne, A., Blanot, L., Trepte, C., Degenstein, D., and Vargas, F.: Major influence of tropical volcanic eruptions on the stratospheric aerosol layer during the last decade, Geophysical Research Letters, 38, https://doi.org/10.1029/2011GL047563, 2011.